Earth Sciences
2021; 10(6): 281-291
http://www.sciencepublishinggroup.com/j/earth
doi: 10.11648/j.earth.20211006.14
ISSN: 2328-5974 (Print); ISSN: 2328-5982 (Online)

Velocity Profile of Turbulent Clear Water Open-Channel Flows: Implication for Suspended Sediment Grains Transport

Lucky Osaro Imagbe

Department of Geology, University of Jos, Jos, Nigeria

Email address:
imagbel@unijos.edu.ng

To cite this article:
Lucky Osaro Imagbe. Velocity Profile of Turbulent Clear Water Open-Channel Flows: Implication for Suspended Sediment Grains Transport. *Earth Sciences.* Vol. 10, No. 6, 2021, pp. 281-291. doi: 10.11648/j.earth.20211006.14

Received: October 4, 2021; **Accepted**: October 30, 2021; **Published**: November 17, 2021

Abstract: Understanding sediment transport process requires adequate knowledge of the mechanism of grains motion which is primarily controlled by flow characteristics including the distribution of time-averaged streamwise velocities, Reynold shear stress distributions as well as the turbulence of flow. Knowledge of the velocity profile in both clear and sediment-laden flows provide clues to understanding this sediment transport mechanism. This paper presents the characterisation of turbulent flow velocity profile based on the physical expression of the mixing length theory as originally proposed by Prandtl, O'Brien and Bagnold, for the prediction of flow interaction with suspended sediment grains. The study utilises the most current flow velocity sampling technology to directly sample flow velocity fluctuations in six cases of open channel flume experiments to characterise the turbulent velocity profile and ascertain the turbulence model's relevance and continuous application in solving sediment grain transport problems. With over 30,000 flow velocity data generated, the analysis demonstrates that, in all six clear water turbulent flows cases investigated, time-averaged velocity versus height is defined in the vicinity of the flow bed by the logarithmic law and well approximated by the turbulence model. Also, modelled and measured vertical streamwise velocities show a significant positive relationship with an R-squared value of almost unity.

Keywords: Sediment Grains, Sediment Transport, Velocity Profile, Mixing-length, Flow Turbulence

1. Introduction

The dynamics of how sediment grains are entrained into flow, transported and deposited have over the years been an active field of research in process sedimentology, marine geology, geomorphology and hydrodynamics. Understanding sediment transport mechanisms provide insights to the processes of erosion and entrainment of sediment grains, as well as clues to predicting the timing and location, where erosion or deposition/accumulation of sediments is anticipated. In particular, understanding sediment transport processes finds useful application in predicting sand distribution and accumulation including their thicknesses and thus of primary interest to hydrocarbon explorationists. Knowledge of sediment transport mechanism helps to mitigate potential environmental and civil engineering problems such as pollution, erosion and flood control, local bed scouring, dredging as well as dam breaching flows among others [13, 46].

However, the mechanism of sediment grains entrainment from parent rocks, their motion and how they are held in suspension has remained a multifaceted active field of research which is yet to be fully explored [42].

In most natural flows, the movement of sediment grains are usually determined by the flow velocity, grain size as well as grain density [2, 23, 29]. Bennett and Best [6], Sharma and Kumar [41] noted that time-averaged flow velocity and turbulence intensity in the distribution of vertical flow velocities proximal to the bed is directly linked to the suspension of sediment grains. This corroborates Bagnold, [4] earlier observation that sediment grains are held in suspension if the rms amplitude of vertical flow velocity fluctuations are greater than the grains fall-velocity. In most sediment-laden fluid-driven

transport, the suspended load is usually proportionately the largest fraction of sediments [20]. Quantifying the amount of sediment grains held in a flow as well as determining the sediment transport rate requires an understanding of the turbulent velocity profile [9, 19]. As sediment grain transport is mainly controlled by flow characteristics including the distribution of time-averaged velocities, Reynold shear stress distributions as well as turbulence intensities [32], the precise characterization of the turbulent velocity profile using a physically based model for predicting the turbulent flow interaction with suspended sediment is vital for understanding sediment grains transport [19, 20, 22, 43]. Under clear-water turbulent flow conditions, the mean velocity profile is described in the vicinity of the wall by the logarithmic law of the wall i.e., flow velocity increases logarithmically with height above the channel bed [45].

Several investigators have developed models based on the vertical distribution of velocity in a flow [1, 7, 27, 51], however, the high uncertainty and unpredictability of the turbulence component in a flow seemed to have limited their practical applicability [23]. In particular, while some models were appropriate for some experimental or field data, the same models could not appropriately fit some other types of measured data [28]. Thus, investigations on velocity distribution in open channel turbulent flow is still very much evolving. Sharma and Kumar, [4] emphasised that the lack of understanding of turbulence and structural characteristics of open channel flows may preclude its wide varying practical applications. However, despite previous numerous works on turbulence and sediment transport in open channel flows, the velocity distribution as well as the vertical velocity profiles of water-sediment mixtures flowing in channels is still not fully understood. Therefore, research in this topical area of sediment transport processes especially is still very fundamental.

The present study aims to improve our understanding of the role of turbulence in sediment transport processes. It evaluates the vertical distribution of streamwise time-averaged velocity in turbulent clear water flows with analysis based on the application of the mixing length turbulence theory as proposed by Prandtl [37].

The next section of this paper will begin with a brief review of the theoretical framework and some of its key assumptions as it relates to this study. Following this, a brief description of the experimental set-up, instrumentation, and measurements will be made, and the results obtained analysed. This paper will be concluded by comparing the measured experimental data to theoretical predictions and show if there is a useful correspondence between these.

2. Theoretical Considerations

The theory outlined below relates to a steady, uniform flow and is therefore applicable to cases where this is a reasonable approximation such as in a river channel (or the body of a long-duration turbidity current) where the width, gradient and direction are slowly varying.

By definition, a uniform flow has a constant thickness throughout and, as a consequence, the flow top has a slope equal to that of the bed floor across which it travels. Furthermore, in a steady flow, there is no acceleration and so friction forces at the base of the flow are exactly balanced by the component of the flow's weight along the sloping base. Hence, for a steady, uniform current

$$\tau_b = -\Delta\rho h\, g\, s \tag{1}$$

where τ_b is basal shear stress, h is the flow thickness, h is the density excess of the flow, g is the acceleration due to gravity and s is the gradient. More generally, similar force balances must exist within the flow itself, i.e. there are internal shear forces of the form

$$\tau_b = -\Delta\rho z\, g\, s \tag{2}$$

where τ_b is produced by shearing between water layers and z is distance from the flow top.

In turbulent flows these internal forces are balanced by Reynold's stresses or eddy stresses and momentum conservation arguments [39], then basal shear stress will be;

$$\tau_b = -\rho\, \overline{u'w'} \tag{3}$$

where ρ is the flow density, u' is the turbulent fluctuation of velocity in the direction of flow and w' is the turbulent velocity fluctuation in the vertical direction.

Throughout this paper, over-bars indicate time-averaging. The velocity fluctuations, in turn, are defined by

$$u = \bar{u} + u',\ v = \bar{v} + v' \ \&\ w = \bar{w} + w' \tag{4}$$

Where u, v and w are the flow velocities in the x, y and z directions.

Combining equations (2) & (3) then gives

$$\overline{u'w'} = z\, g'\, s \tag{5}$$

where g' ($=g\Delta\rho/\rho$) is known as the reduced gravity.

We can now introduce a shearing velocity, u_*, defined by

$$\tau_b = -\rho u_*^2 \tag{6}$$

This simply recasts the basal friction of the flow in terms of a parameter with the dimensions of velocity but, as we'll see, this is a useful transformation. It follows from equations (1), (3) and (6) that

$$u_*^2 = hg's. \tag{7}$$

and

$$u_*^2 = \overline{u'w'}_0 \tag{8}$$

The mixing length theory of turbulence describes the distance a sediment grain will move without necessarily losing its original character. It expresses how fluctuations in flow velocity is used to predict the amount of turbulence needed to support the movement and suspension of sediment

grains in a steady uniform flow. Proposed by Prandtl [37], the "mixing-length" refers to the average distance that a fluid particle can move freely without collision and momentum exchange. It also describes the flow height which characterise interchanges of fluid particles in a turbulent flow as well as the distance the particle could keep its original characteristics before assuming that of the surrounding fluid.

The mixing length theory as originally proposed by Prandtl, [15] as presented by Duncan [37] utilizes u_* and predicts a logarithmic velocity profile in turbulent flows (the "law-of-the-wall") given by

$$u = (u_*/\kappa)\ln(Z/z_0) \tag{9}$$

where k is von Karman's constant, Z is distance above the flow base and z_0 is a constant related to the roughness at the flow-base.

The final component of theory relates the velocities discussed above to grain suspension. Turbulent suspension occurs due to the vertical velocity fluctuations, near the flow base, which exceed the fall velocity [4]. Characterizing these fluctuations by their root mean square (RMS) value then gives a suspension criterion of

$$\sqrt{\overline{w'^2}}_0 \gtrsim \mathrm{U_{fall}} \tag{10}$$

where U_{fall} is the fall speed of the particles under consideration.

However, in an un-instrumented flow, the RMS velocity fluctuations are not known, and the assumption is usually made that turbulence is approximately isotropic so that

$$\overline{w'^2} \approx \overline{u'w'}. \tag{11}$$

and hence, from equation (8),

$$\mathrm{U_{fall}} \lesssim u_*. \tag{12}$$

3. Method: Experimental Description

The synopsis of the experimental procedure applied in this study is presented below.

The flume tank facility

The experimental facility was located at Sorby Fluid Dynamics Laboratory at the University of Leeds. The facility includes a tilting rectangular glass-sided flume, 8.5m long, 0.34m deep and 0.3m wide (figure 1), which provided clear view of the flow and allowed high-speed photography as well ease in taking measurement. The other parts of the flume, particularly the frames, were made of corrosion resistant steel (see figure 1).

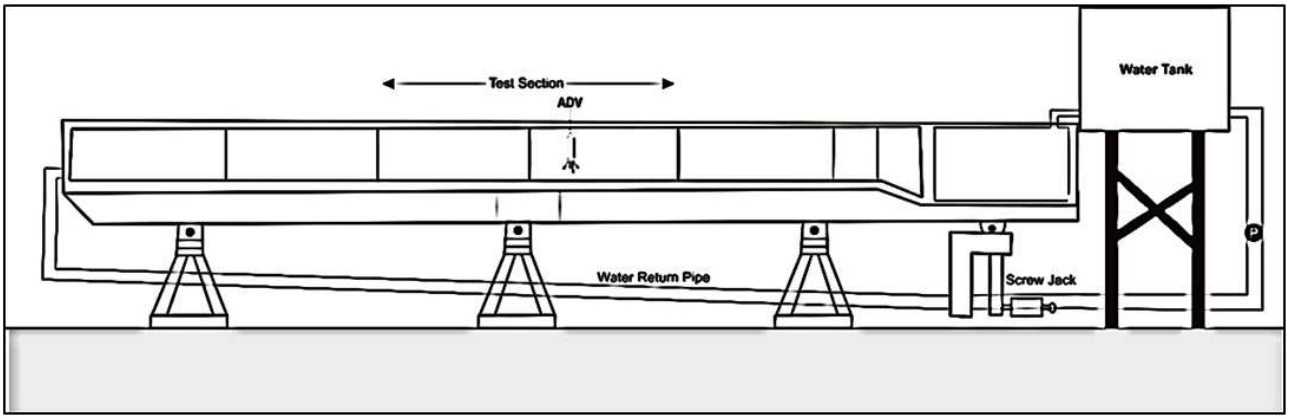

Figure 1. *Schematic diagram of the experimental set up and laboratory flume used in this research.*

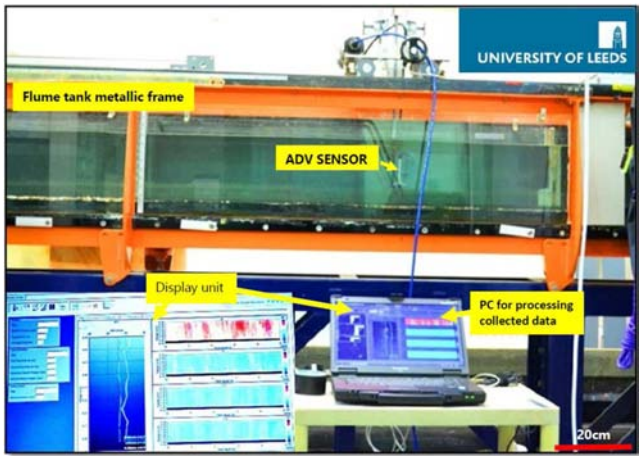

Figure 2. *The Flume (The Measurement and Observation section as well as the instrumentation).*

A Hydrostat centrifugal pump was fitted to the flume tank to drive clear water into the flume which was recirculated through the flume via a return PVC pipe of 0.20 m diameter, placed below the flume tank. The re-circulating flume was necessary to maintain uniform flow of water circulation in the flume. The flow discharge rate into the flume tank was monitored using an ABB electromagnetic flow meter which was controlled via an inverter control unit which governed the discharge rate and flow velocity. A pack of stainless-steel pipes of 2.50 cm radius were placed at the upstream end of the flume tank to prevent an occurrence of vortex flow. Water temperature was an average of 20±2°C.

The flume was instrumented with a three-dimensional (3-C) Acoustic Doppler Velocimeter (ADV) measuring system, which was positioned on the centre of the flume, about 4.2m from the downstream end of the flume and all

measurements taken at the centreline of the cross section (see figure 2).

Six experimental cases were designed for the flow experiment with unique conditions such as varying discharge rate, flow height/thickness, type of flume floor (roughness) as well as the slope of the flume.

The experiment began with clear water being pumped from an overhead tank into the flume and allowed to recirculate until a uniform steady flow was achieved. Care was exercised to avoid possible hydraulic jump/vortex flow occurring along the flow path and especially at the upstream end of the flume by maintaining a suitable discharge rate. A hydraulic jack beneath the flume was used to tilt the flume and adjust the slope of the flume.

The initial flow speed was calculated from the volumetric discharge with respect to the cross-sectional area. This was varied for the different experimental flow cases.

An outline of the flow condition is listed in Table 1 below.

Table 1. *Summary of flume hydraulic data for all six experimental cases.*

Flow conditions	Case 1	Case 2	Case 3	Case 4	Case 5	Case 6
Type of floor	Concrete	Concrete	Gravel	Gravel	Gravel	Gravel
Flow height to roughness (m)	0.92	0.18	0.192	0.192	0.14	0.14
Flow area (m^2)	0.058	0.054	0.058	0.058	0.042	0.042
Flume average slope	0.053	0.071	0.079	0.088	0.132	0.141
Mean discharge rate (l/s)	21.6	39.6	24.6	31.3	21.6	33.19
Mean discharge rate (m^3/s)	0.022	0.04	0.025	0.031	0.022	0.033
Mean flow velocity (m/s)	0.36	0.551	0.333	0.512	0.443	0.616

The Acoustic Doppler Velocimetry

Acoustic Doppler Velocimeter (ADV) is one of the most recent devices for flow velocity and turbulence measurements [8, 18, 24, 36, 40]. Unlike the previous ADVs with 3 receivers, the Vetrino-II ADV used for this experiment has 4 heads which consist of 4 receivers positioned at x, y, z_1 and z_2 directions, with beams 1 and 3 recording data in the downstream (u) and vertical (z_1) velocities, beams 2 and 4 record data of the cross stream (v) and vertical (z_2) velocities.

The addition of the 4th probe head allowed the Vectrino-II to record two vertical velocities to provide a greater accuracy in the measurements. This also allowed the device to record data at a higher frequency (100Hz) without compromising the quality of the data. It is worthy to note that the experiment made use of the latest version of the Vectrino profiler ADV (Vectrino II), which was configured to simultaneously measure flow velocities at 17 different distances from the transmitter at each of the chosen probe position as set with the trolley which was vertically beneath the transducer (oriented perpendicular to the flume bed). The 17 multiple positions were performed to generate multiple overlapping vertical profiles so that a single time-averaged profile encompassing most of the water column could be formed.

The velocity profiles were constructed by moving the Vectrino profiler in 10 mm increments from 50 mm above each bed surface until the water surface began to interfere with the transmitter. At each location, velocities were sampled at 100 Hz for 300 seconds. According to Chanson et al., [10], raw ADV velocity data do not represent true flow turbulence unless it has been post-processed to remove spikes, Doppler noise and any filtering effects arising from the ADV sampling method. In the experiments, the acquired flow velocity data were post-processed in-house by the University of Leeds Sorby Laboratory team using an intelligent correlation threshold filter comprising of a phase unwrapping algorithm and the phase space threshold spike filter (see [44] for more details).

4. Data Analysis, Results, and Discussion

In this section, a summary of the experimental results, analysis and discussion are presented.

Instantaneous streamwise velocity- time series

Figures 4 and 5 show the instantaneous streamwise velocity-time series for turbulent flows over both smooth concrete and rough gravel floors for the flume experiments. The instantaneous streamwise velocity, here implies the sum of the time-averaged velocity and the fluctuating velocity components in the streamwise direction (see equation 4). Separate profiles correspond to different heights of the velocity sampling device (ADV) above the tank floor and different experimental flow conditions.

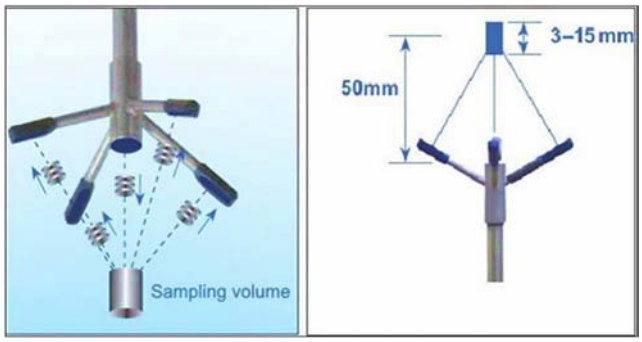

Figure 3. *The ADV probe with transducer, receiver, and sampling volume. Adapted from Nortek [34].*

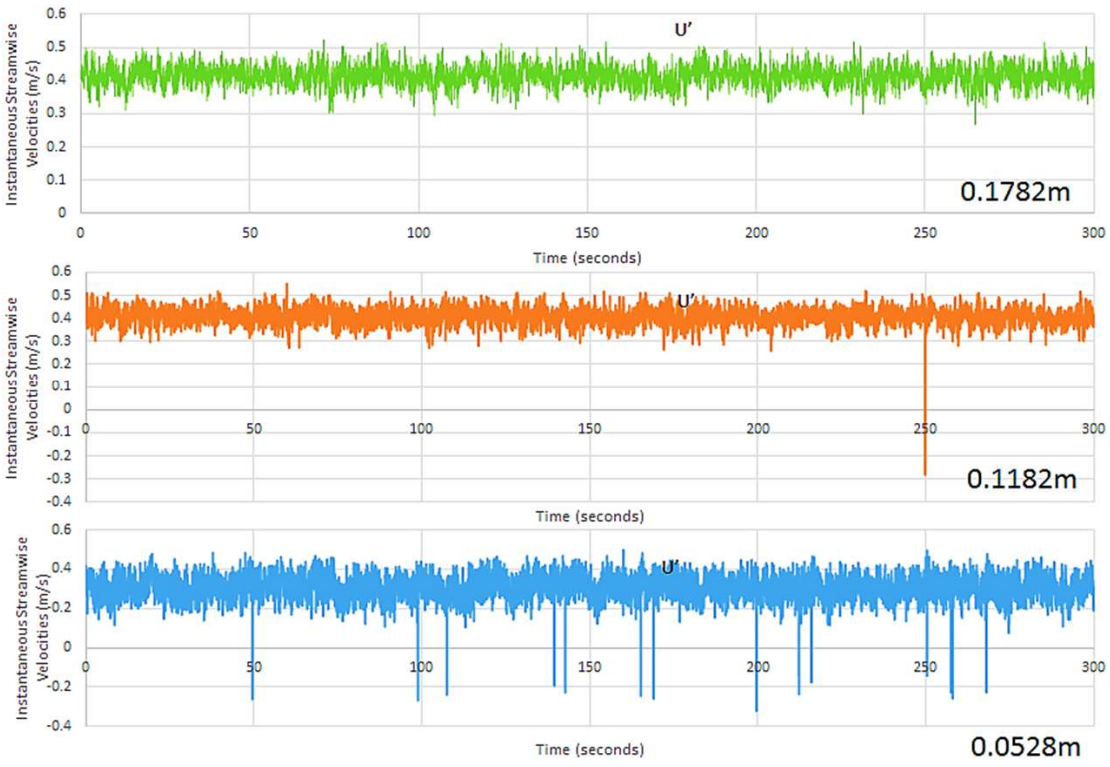

Figure 4. *Instantaneous velocity –time series for case 1 (smooth concrete floor).*

Velocity-depth profiles

Velocity profiles for all six clear water flow cases as computed based on averaging of the instantaneous streamwise velocity measurements are presented in figures 6-11 below. The profiles show a velocity maximum near the water surface and a velocity minimum near the base of flow. The velocity maximum usually occurs close to the bed near the density maximum and an upwards decreasing velocity until near zero at the top (figure 1). The height of the maximum velocity is controlled by the ratio of the drag forces at the upper and lower boundaries [25, 26].

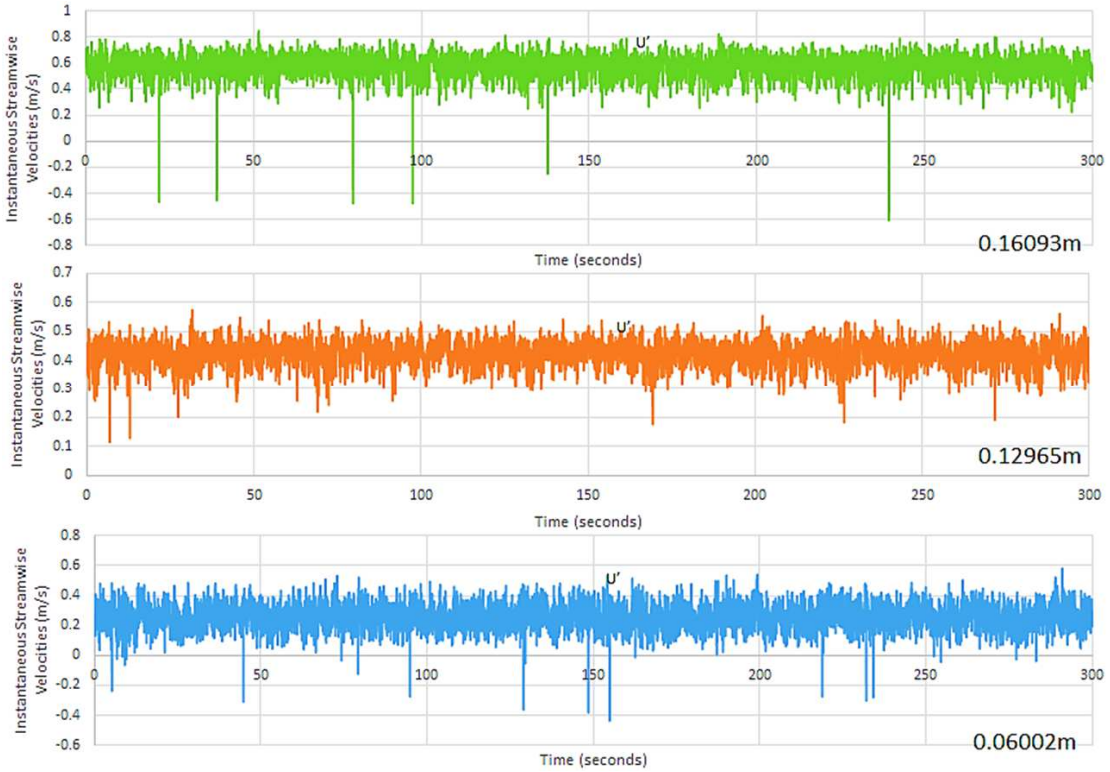

Figure 5. *Instantaneous velocity –time series for case 1 (rough gravelly floor).*

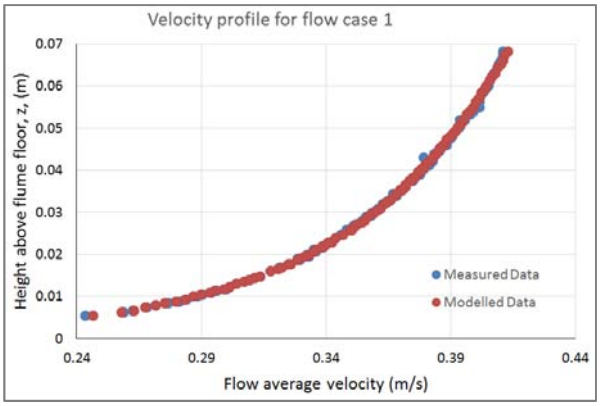

Figure 6. *Velocity profile for flow case 1 (from measured and modelled dataset).*

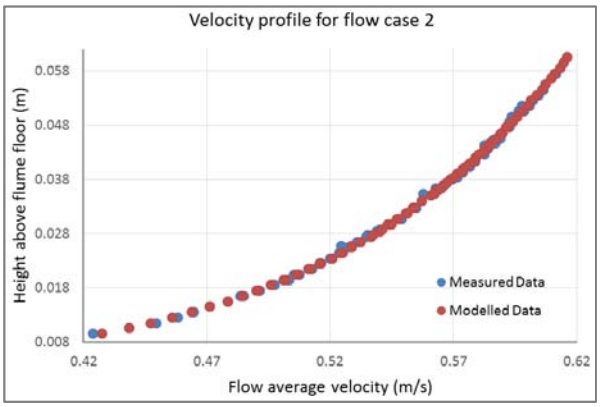

Figure 7. *Velocity profile for flow case 2 (from measured and modelled dataset).*

Measured and modelled flow velocities

Experimentally derived mean flow velocity data for all six flow cases were matched with modelled velocities to determine how well both data agree as presented in figures 12-17.

Due to the large data involved, the *Regression* package in *Excel* was used to calculate the bed shear stress estimates. A regression statistical analysis including the R-squared and P-values obtained using excel analytical tool also confirmed a significant positive relationship between both flow velocities.

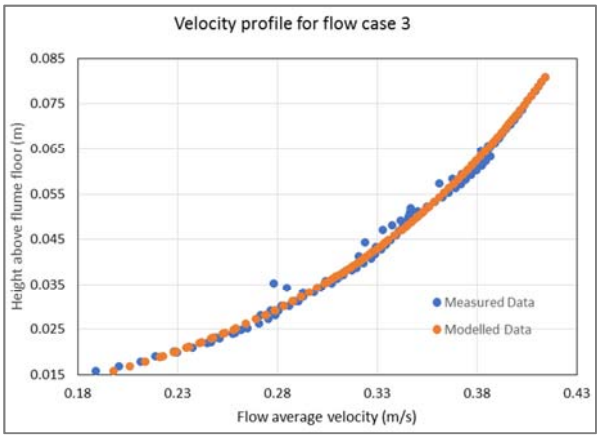

Figure 8. *Velocity profile for flow case 3 (from measured and modelled dataset).*

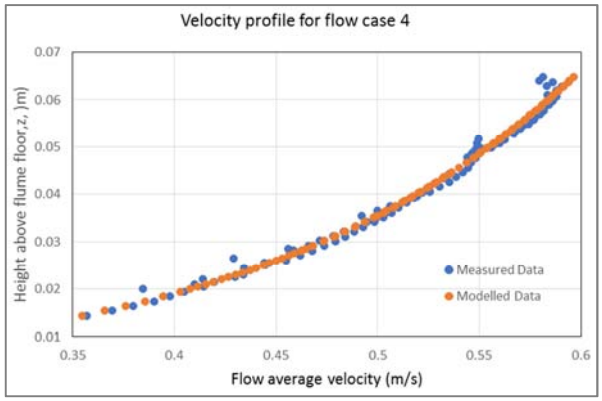

Figure 9. *Velocity profile for flow case 4 (from measured and modelled dataset).*

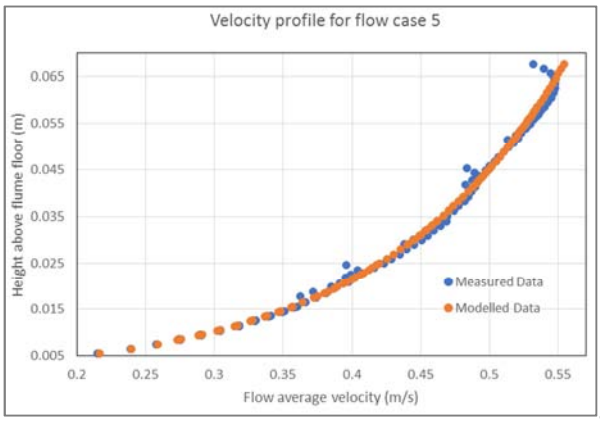

Figure 10. *Velocity profile for flow case 5 (from measured and modelled dataset).*

Using the Law-of-the-Wall approach, modelled velocities were estimated with flow velocities at different flow heights measured and plotted against flow height and then using the fitting procedure, estimates of shear velocities and roughness were derived from the slope and intercept of the computed regression equation.

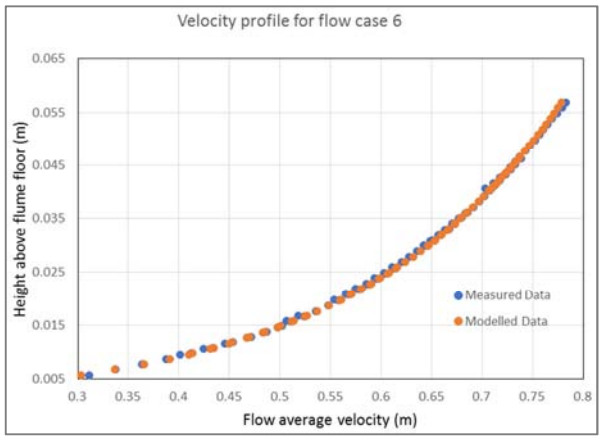

Figure 11. *Velocity profile for flow case 6 (from measured and modelled dataset).*

For a uniform flow, where there is no sediment transport

(as in this clear water experiment), it has been established that von Karman's constant κ varies from 0.16 to 0.41. (Table 3). The value of κ is now often reported to be significantly smaller than the canonical value of 0.40 [12, 14, 17, 52].

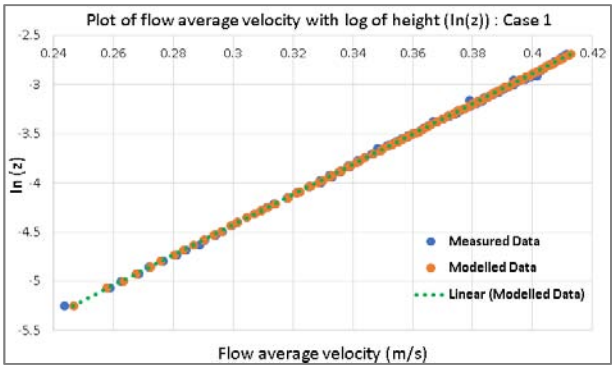

Figure 12. *Plot of average flow velocity vs log of height, In (z), for flow case 1.*

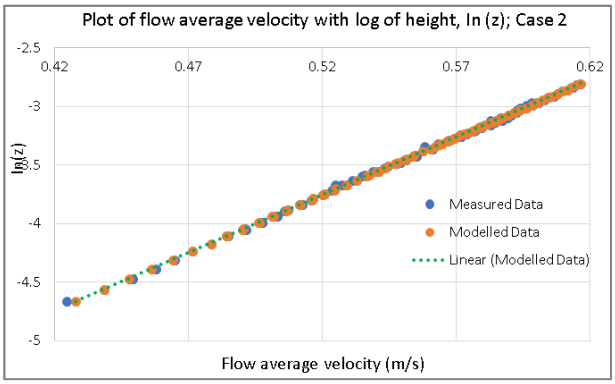

Figure 13. *Plot of average flow velocity vs log of height, In (z), for flow case 2.*

Thus, an assumed lower, κ value of 0.29 (similar to lower κ-values used by other authors as in table 3) was used in the data analysis to minimise mismatch between the Law-of-the-Wall and Reynolds stresses.

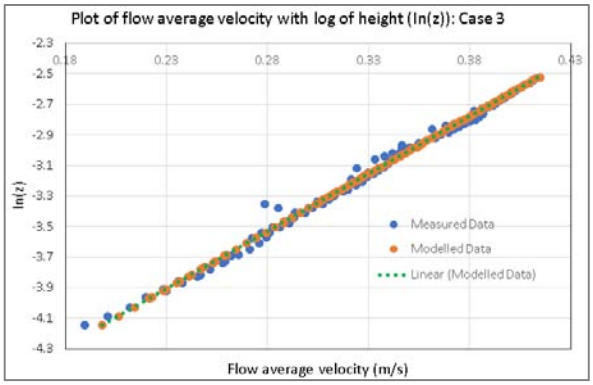

Figure 14. *Plot of average flow velocity vs log of height, In (z), for flow case 3.*

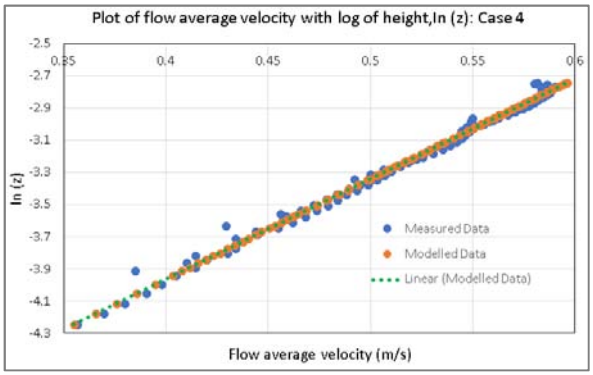

Figure 15. *Plot of average flow velocity vs log of height, In (z), for flow case 4.*

Table 2. *Summary of Regression statistics of flow velocity data for all six experimental cases.*

Regression statistics	Case 1	Case 2	Case 3	Case 4	Case 5	Case 6
Observations	112	85	112	100	96	80
Multiple R	0.99978	0.99962	0.997	0.995893	0.997855	0.99968
R-Squared	0.99955	0.99925	0.99402	0.991802	0.995715	0.99935
Standard Error	0.00086	0.00127	0.00443	0.005615	0.005598	0.00303
P-Value	3.10E-18	2.10E-131	3.80E-124	4.80E-104	4.10E-113	3.70E-126

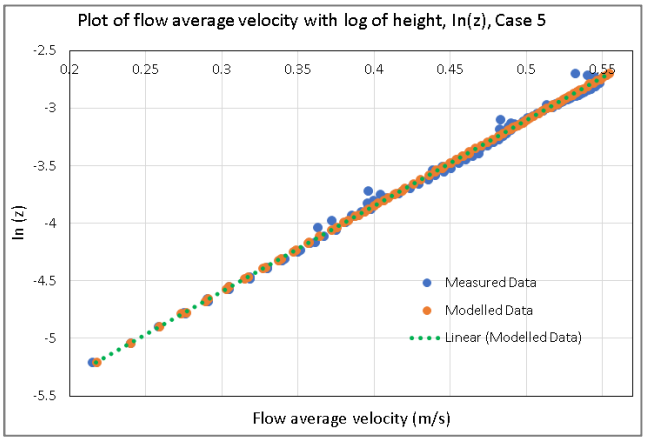

Figure 16. *Plot of average flow velocity vs log of height, In (z), for flow case 5.*

Table 3. *Summary of some von Karman's constant values available in the literature.*

Reference	Reported value
Von Karman (1930)	0.4
Wang and Larsen (1994)	0.16
Einstein and Chien (1955)	0.168-0.406
Vanoni and Nomicos (1960)	0.209-0.384
Andreas et al. (2006)	0.39
Gust and Southard (1983)	0.28
Mckeon et al. (2004)	0.3
Present study (2021)	0.29

Flow velocities at different depths re-plotted against log of flow height (In(z)) as presented in figures 12-17 below show straight lines (see equation 9) and give similar information as earlier curves (figures 6-11). All plots showed significant agreement between measured and modelled velocities.

Turbulence and Sediment Grain Suspension

Bed Surface Roughness

Bed surface roughness can be produced by bed forms (ripples and mega ripples) as well as by varying sizes of individual sediment grains. The roughness of a bed significantly contributes to turbulence in a flow [33]. In this study, the estimated bed surface roughness height, z_0, of the two types of slabs used in the experiments include smooth concrete (D_{50} < 0.5mm) for flow cases 1-2 and gravel (D_{50} approx. 3.0mm) for flow cases 3-6. In the turbulence model, z_0 represents the surface roughness length or height, where the instantaneous velocity equals to zero. The modelled roughness length, z_0, was derived from the fitting of the velocity profiles. The relationship between z_0 and the size of the roughness element which provided a measure of the bed grain size as derived by Raudkivi [38] is presented in equation (9). The roughness estimates and their uncertainties are presented in table 4 below.

Table 4. *Estimates of roughness lengths for surfaces used in the experiment.*

Floor type	Case 1	Case 2	Case 3	Case 4	Case 5	Case 6
	Concrete	Concrete	Gravel	Gravel	Gravel	Gravel
Flow thickness	0.192	0.18	0.192	0.192	0.14	0.14
Roughness (m)	0.00012	0.00014	0.00257	0.00157	0.00159	0.00162
Uncertainty	0.00003	0.00005	0.00023	0.00014	0.00008	0.0004

It is expected that rougher floors should have higher values of z_0 and consequently, produce greater turbulence. To test this, the roughness length, z_0, was estimated from the log-profile method, through a best fit and κ-value adjusted to 0.29 (to minimise the difference between the basal stress from Law-of-the-Wall and the Reynolds stress (see table 4 and figure 18). Clearly, from the results, gravel has a higher z_0 than concrete and there is a clear dichotomy between the gravel cases with z_0 ~ 0.002 m and the concrete-base case with z_0 ~ 0.0001m. However, these results also show that roughness elements, x, is greater than the roughness length, z_0, which interestingly confirms similar observations by Raudkivi [38].

Drag coefficient

The drag coefficient, C_D, of the flows was estimated using expression provided by Waltham [49]. Table 5 below provides the estimates as well as the comparison of drag coefficient, C_D, of the flows over concrete and rough floors from the Law-of-the-Wall and the Reynolds shear stress methods.

Table 5. *Comparison of CD estimates from LoW and RSS.*

Drag coefficient, C_D estimates	Concrete	Gravel
LoW	2.0405	5.8433
RSS	2.4364	5.3418

It is clear from the results as well as figures 19 and 20 that both methods produce similar estimates of drag coefficient, C_D, and are thus reliable. As expected, a key observation from these figures confirms that the estimates of the drag coefficients for the rough gravel surfaces are higher than that of the smooth concrete surface. Table 5 also shows that that the basal shear stress of the rough gravelly floor is higher than that of the smooth concrete floor. This confirmed earlier works of Poggi et al.,[35], suggesting that shear stress should increase with bed roughness. Chien and Chew [11], in their experiment also found that shear velocity in marble bed was higher compared to sand bed due to the relative roughness of the marble bed. The implication is that rough beds create more flow turbulence and facilitate the suspension of sediment grains in a moving flow. Mazumder et al., [30] investigation, also revealed that higher bed roughness significantly controls the size distribution of suspended load and accounts for keeping sand-size sediment grains in suspension in a low-concentration flow.

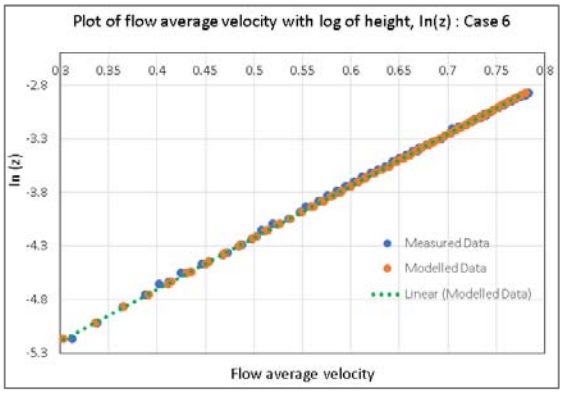

Figure 17. *Plot of average flow velocity vs log of height, In (z), for flow case 6.*

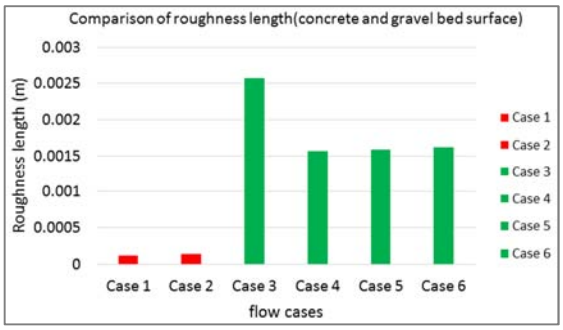

Figure 18. *Comparison of roughness length (concrete and gravelly floors).*

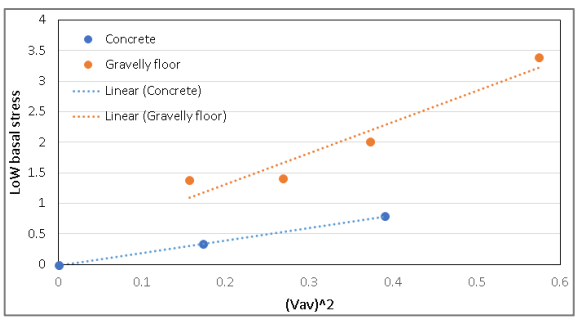

Figure 19. *Drag Coefficient estimates from Law-of-the-Wall. The gradients of the straight line give the estimate of C_D.*

The foregoing experimental results all concern relationships between different estimates of turbulent fluctuation magnitude. However, the focus has been on the capacity of a turbulent flow to maintain sediment particles in suspension. The physics of turbulent flows as described by Andreas et al., [3], also confirmed that suspension of sediment grains can only occur when the vertical velocity fluctuations near the flow base exceed the grains fall velocity. Characterizing these fluctuations by their root mean square *(rms)* value then gives a suspension criterion as in equations (10 & 11).

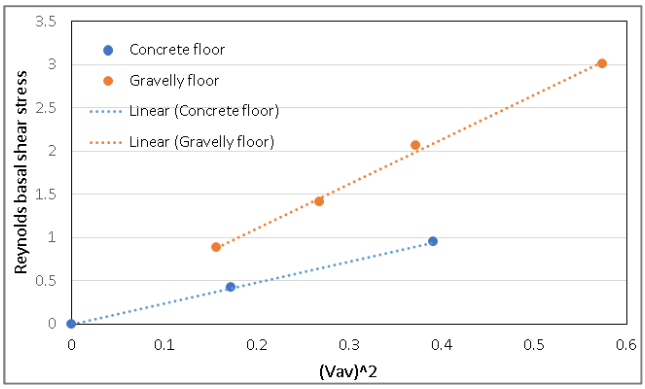

Figure 20. *Drag Coefficient estimates from Reynold stress. The gradients of the straight line give the estimate of* C_D.

5. Conclusion

Based on the experimental and analytical evidence presented in this paper, one can conclude that:

Modern measurements of flow turbulence confirm that shear stresses within a steady, uniform water flow are balanced by eddy stresses of the kind predicted by Reynolds [39].

Mixing-length theory of turbulent suspension of sediment grains work well within a steady, uniform flow and, hence, the law of the wall provides a good model of the vertical velocity profile. However, the results of this study have also demonstrated that the theory is applicable to unsteady, non-uniform flows such as rivers.

Time-averaged velocity versus height is well approximated by the Von Karman turbulence model. This is well illustrated by Figures 6-11.

Reports, from earlier studies, that von Karman's constant, is not after all universal but varies and can be significantly smaller than the widely accepted value of 0.41, are strongly supported. Based on the clear water flow experiments, a κ value of 0.3±0.02 is recommend for low concentration flows. Low values for κ have been reported by several other researchers and so the derived κ value of 0.29 in this research is not unreasonable.

Basal shear stress calculated from the Von-Karman turbulence model agree with the Reynold's estimates provided a von Karman constant of 0.29 is used.

Modelled and measured flow velocities show a significant positive relationship with an R-squared value of almost unity.

Basal shear stress estimates obtained from the Law-of-the-Wall and Reynolds stress show reasonable agreement confirming the reliability of the Mixing Length turbulent suspension theory. Drag coefficient estimates obtained from both methods also show a significant correlation.

The turbulent suspension theory has been supported by the good fits of measured data to predictions of the Law-of-Wall, good fits to the predictions of RANS as well as the good fits of stress=Cd.v^2.

Flow turbulence is controlled by the roughness at the flow base and the size of this coefficient is greater than the roughness element, z_0, which interestingly confirms similar observations by Raudkivi [38]. Drag coefficient estimated from Waltham, [49] also confirms that drag due to friction on gravelly surfaces exceeds that of the smooth floor used in the flume experiment.

Turbulence of a flow therefore is attenuated by increased bed surface roughness underlying the flow.

Acknowledgements

The data for this paper is from the author's PhD research (Applied Sedimentology) in the department of Earth Sciences, Royal Holloway University of London, United Kingdom. The author is grateful to the Petroleum Technology and Development Fund (PTDF) of Nigeria for the award of a PhD Scholarship to the author which enabled the author to successfully carry out his research at Royal Holloway, University of London.

The author would also like to thank the fluid dynamics laboratory team especially Dr Gareth Keevil and Dr Robert E. Thomas, of the University of Leeds and University of Hull respectively for their help with the flume experiments.

References

[1] *Absi, R.* An ordinary differential equation for velocity distribution and dip-phenomenon in open channel flows. Journal of Hydraulic Research, 2011. 49 (1): 82–89.

[2] *Allen, J. R. L.* Principles of physical sedimentology. George Allen & Unwin Ltd., London. 1985.

[3] *Andreas, E. L., Claffey, K. J., Jordan, R. E., Fairall, C. W., Guest, P. S., Persson, P. O. G. and Grachev, A. A.,* Evaluations of the von Kármán constant in the atmospheric surface layer. Journal of Fluid Mechanics. 2006. 559, pp. 117-149.

[4] *Bagnold R. A*. An approach to the sediment transport problem from general physics. US government printing office; 1966.

[5] *Balachandar, S. and Eaton, J. K.* Turbulent dispersed multiphase flow. Annual Review of Fluid Mechanics. 2010. 42, 111–133.

[6] *Bennett, S. J., and Best, J. L.* Particle size and velocity discrimination in a sediment-laden turbulent flow using phase Doppler anemometry. 1995. 505-511.

[7] *Bialik R. J.* Numerical study of near-bed turbulence structures influence on the initiation of saltating grains movement. J Hydrol Hydromech. 2013. 61 (3): 202–207.

[8] *Biron, P. M., Robson, C., Lapointe, M. F., and Gaskin, S. J.* Comparing different methods of bed shear stress estimates in simple and complex flow fields: Earth Surface Processes and Landforms. 2004. v. 29, no. 11, p. 1403-1415.

[9] *Castro-Orgaz, O., Giráldez, J. V., Mateos, L. and Dey, S.* Is the von Kármán constant affected by sediment suspension? J. Geophys. Res. 2012. 117.

[10] *Chanson, H., Trevethan, M., and Koch, C.* Discussion of "Turbulence measurements with acoustic Doppler velocimeters" by Carlos M. Garcia, Mariano I. Cantero, Yarko Nino, and Marcelo H. Garcia: Journal of Hydraulic Engineering. 2007. v. 133, no. 11, p. 1283-1286.

[11] *Chen, X., and Chiew, Y.-M.* Response of velocity and turbulence to sudden change of bed roughness in open-channel flow: Journal of Hydraulic Engineering. 2003. v. 129, no. 1, p. 35-43.

[12] *Darby, S. E., and Peakall, J.* Modelling the equilibrium bed topography of submarine meanders that exhibit reversed secondary flows: Geomorphology. 2012. v. 163, p. 99-109.

[13] *Dewals, B. J., Rulot, F., Erpicum, S., Archambeau, P., and Pirotton, M.* Long term sediment management for sustainable hydropower. Comprehensive Renewable Energy. 2010b. Volume 6-Hydro Power, A Sayigh, ed., Elsevier, Oxford.

[14] *Dorrell, R., Darby, S., Peakall, J., Sumner, E., Parsons, D., and Wynn, R.* The critical role of stratification in submarine channels: Implications for channelization and long runout of flows: Journal of Geophysical Research: Oceans. 2014. v. 119, no. 4, p. 2620-2641.

[15] *Duncan, W. J.* An elementary treatise on the mechanics of fluids, Arnold 1960.

[16] *Einstein, H., and Chien N.,* Effects of heavy sediment concentration near the bed on velocity and sediment distribution, Mo. River Div. Sediment Ser. 8, Inst. of Eng. Res. 1955. Univ. of Calif., Berkeley, Calif.

[17] *Felix, M., Peakall, J., and McCaffrey, W.* Relative importance of processes that govern the generation of particulate hyperpycnal flows: Journal of Sedimentary Research. 2006. v. 76, no. 2, p. 382-387.

[18] *García, C. M., Cantero, M. I., Niño, Y., and García, M. H.* Turbulence measurements with acoustic Doppler velocimeters: Journal of Hydraulic Engineering. 2005. v. 131, no. 12, p. 1062- 1073.

[19] *Garcia, M. H.* Sediment transport and morphodynamics, in Sedimentation Engineering, ASCE Manuals and Rep. on Eng. Pract. 2008. vol. 110, chap. 2, pp. 21–162, Am. Soc. Civ. Eng., Reston, Va.

[20] *Gust, G., and Southard, J. B.* Effects of weak bed load on the universal law of the wall: Journal of Geophysical Research: Oceans. 1983. v. 88, no. C10, p. 5939-5952.

[21] *Hill, P. S., Nowell, A. R. M. and Jumars, P. A.* Flume evaluation of the relationship between suspended sediment concentration and excess boundary shear stress, J. Geophys. Res. 1988. 93 (C10), 12, 499–12, 509.

[22] *Jain, P. and Ghoshal, K.* An explicit expression for velocity profile in presence of secondary current and sediment in an open channel turbulent flow. Canadian Journal of Civil Engineering. 2021. 48 (1), pp. 52-61.

[23] *Khosravi K, Chegini AH, Cooper JR, Daggupati P, Binns A, Mao L.* Uniform and graded bed-load sediment transport in a degrading channel with non-equilibrium conditions. International Journal of Sediment Research. 2020 1; 35 (2): 115-24.

[24] *Kim, S.-C., Friedrichs, C., Maa, J. Y., and Wright, L.* 2000. Estimating bottom stress in tidal boundary layer from acoustic Doppler velocimeter data: Journal of Hydraulic Engineering, v. 126, no. 6, p. 399-406.

[25] *Kneller, B., Bennett, S., and McCaffrey, W.* Velocity and turbulence structure of density currents and internal solitary waves: potential sediment transport and the formation of wave ripples in deep water: Sedimentary Geology. 1997. v. 112, no. 3-4, p. 235-250.

[26] *Kneller, B., Nasr-Azadani, M. M., Radhakrishnan, S., and Meiburg, E.* Long-range sediment transport in the world's oceans by stably stratified turbidity currents: Journal of Geophysical Research. (2016): Oceans.

[27] *Kundu S, Ghoshal K.* An analytical model for velocity distribution and dip-phenomenon in uniform open channel flows. Int J Fluid Mech Res. 2012. 39 (5): 381–395.

[28] *Kundu, S., Kumbhakar, M. and Ghoshal, K.* Reinvestigation on mixing length in an open channel turbulent flow. Acta Geophysical. 2018, *66* (1), pp. 93-107.

[29] *Leeder, M. R.* Sedimentology: Processes and products. London: George Allen & Unwin Ltd. 1982.

[30] *Mazumder, B., Ghoshal, K., and Dalal, D.* Influence of bed roughness on sediment suspension: experimental and theoretical studies: Journal of Hydraulic Research, 2005. v. 43, no. 3, p. 245-257.

[31] *McKeon, B. J., Li, J., Jiang, W., Morrison, J. F. & Smits, A. J.* Further observations on the mean velocity distribution in fully developed pipe flow. J. Fluid Mech. 2004. 501. 135–147.

[32] *Miguntanna, N. S., Moses, H., Sivakumar, M., Yang, S. Q., Enever, K. J. and Riaz, M. Z. B.* Re-examining log law velocity profile in smooth open channel flows. Environmental Fluid Mechanics. 2020. pp. 1-34.

[33] *Nakagawa, H., Nezu, I. and Ueda, H.* Turbulence of open channel flow over smooth and rough beds. In Proceedings of the Japan Society of Civil Engineers. 1975. No. 241, pp. 155-168.

[34] *Nortek, A*. Vectrino velocimeter user guide. 2004. (Rev. C), Norway.

[35] *Poggi, D., Porporato, A., and Ridolfi, L.* Analysis of the small-scale structure of turbulence on smooth and rough walls: Physics of Fluids. 2003. v. 15, no. 1, p. 35-46.

[36] *Pope, N., Widdows, J., and Brinsley, M.* Estimation of bed shear stress using the turbulent kinetic energy approach—a comparison of annular flume and field data: Continental Shelf Research. 2006. v. 26, no. 8, p. 959-970.

[37] *Prandtl L.* Bericht uber untersuchungen zur ausbgebilddeten turbulenz. Zeitschrift fur Angewandte Mathematik und Mechanik. 1925 (2): 136-139.

[38] *Raudkivi, A. J.* Loose boundary hydraulics, CRC Press. 1998.

[39] *Reynolds, O*. On the dynamical theory of incompressible viscous fluids and the determination of the criterion. Philosophical Transactions of the Royal Society of London. 1895. 186, pp 123-164.

[40] *Rowiński, P., Aberle, J., and Mazurczyk, A*. Shear velocity estimation in hydraulic research: Acta Geophysica Polonica. 2005. v. 53, no. 4, p. 567-583.

[41] *Sharma, A., and Kumar, B*. Comparison of flow turbulence over a sand bed and gravel bed channel. *Water Supply*. 2021.

[42] *Sindelar C, Smart G*. Transition flow in step-pool systems: Pressure distributions and drag forces. Journal of Hydraulic Engineering. 2016 1; 142 (10).

[43] *Smith, J. D. and McLean, S. R.* Spatially averaged flow over a wavy surface. Journal of Geophysical research, 1977. 82 (12), pp. 1735-1746.

[44] *Thomas, R. E., and Mclelland, S. J.* The impact of macroalgae on mean and turbulent flow fields: Journal of Hydrodynamics. *2015*. Ser. B, v. 27, no. 3, p. 427-435.

[45] *Uchida, T. and Fukuoka. S*. Quasi-3D two-phase model for dam-break flow over movable bed based on a non-hydrostatic depth-integrated model with a dynamic rough wall law. *Advances in Water Resources* 129. 2019. 311-327.

[46] *Van Rijn L. C.* Unified view of Sediment Transport by Currents and Waves. I: Initiation of Motion, Bed Roughness and Bed-Load Transport. Journal of Hydraulic Engineering. 2007. 133 (6), 649-667.

[47] Vanoni. A., and Nomicos, G. N. Resistance properties of sediment-laden streams: Transactions of the American Society of Civil Engineers. 1960. v. 125, no. 1, p. 1140-1167.

[48] *Von Karman, T*. Some aspects of the turbulence problem. Mech. Eng., 1930. 407-412.

[49] *Waltham, D.* Slope control on submarine channel widths. *Journal of Sedimentary Research*. 2008b *78* (5), pp. 317-322.

[50] *Wang, Z., and Larsen, P.* Turbulent structure of water and clay suspensions with bed load: Journal of Hydraulic Engineering. 1994. V. 120. no. 5, p. 577-600.

[51] *Yang S. Q*. Mechanism for initiating secondary currents in channel flows. Can J Civ Eng. 2009. 36 (9): 1506–1516.

[52] *Yin, D., Peakall, J., Parsons, D., Chen, Z., Averill, H. M., Wignall, P., and Best, J.* Bedform genesis in bedrock substrates: Insights into formative processes from a new experimental approach and the importance of suspension-dominated abrasion: Geomorphology. 2016. v. 255, p. 26-38.